

# Softened CH Stretching Vibration of a Long-Chain *n*-Alkane, *n*-C<sub>44</sub>H<sub>90</sub>, Physisorbed on a Ag(111) Surface: An Infrared Reflection Absorption Spectroscopic Study

Masato Yamamoto,<sup>\*,†,‡,§</sup> Yoko Sakurai,<sup>†</sup> Yoshinobu Hosoi,<sup>†</sup> Hisao Ishii,<sup>†</sup> Kotaro Kajikawa,<sup>\*,†,⊥</sup> Yukio Ouchi,<sup>†</sup> and Kazuhiko Seki<sup>†,‡</sup>

Department of Chemistry, Graduate School of Science, Nagoya University Furocho, Chikusa-ku, Nagoya 464-8602, Japan, and Research Center for Materials Science, Nagoya University, Furocho, Chikusa-ku, Nagoya 464-8602, Japan

Received: December 23, 1999; In Final Form: May 3, 2000

A long-chain *n*-alkane, tetratetracontane (*n*-C<sub>44</sub>H<sub>90</sub>), adsorbed on Ag(111) was studied by infrared reflection absorption spectroscopy. The first layer is physisorbed on the surface and assumes a “flat-on” structure with the molecular plane formed by the carbon atoms parallel to the surface. This structure gives CH stretching vibration bands at 2907 and 2814 cm<sup>-1</sup>, which are attributed mainly to the CH bonds in the upper side of the molecular plane and those in the vicinity of the Ag(111) surface, respectively. These frequencies are lower than those for the normal stretching modes of a methylene group, and this difference is ascribed to the interaction between the CH bonds on the metal side and the Ag surface. This “softening” of the CH bond in contact with the surface was explained by the interaction between the dipole and the image dipole induced in the metal substrate, and this frequency shift of the CH stretching vibration was simulated by electrodynamic calculations.

## I. Introduction

*n*-Alkanes are a basic class of organic compounds, and many studies have been performed in various states, including adsorbed states on metals. For example, the two-dimensional geometries of *n*-octane and *n*-hexane on Ag(111) and Pt(111) crystal surfaces were studied by low-energy electron diffraction (LEED),<sup>1,2</sup> and these short *n*-alkanes were found to be physisorbed on the surfaces in ordered structures. On the other hand, few studies<sup>3–8</sup> have been reported on the vibrational spectra for long-chain *n*-alkanes or their long-chain limit, polyethylene, in the vicinity of metal surfaces. Most of these studies did not examine the detailed mechanism of the spectral changes caused by interaction with the metal surface.

Our group has studied the electronic structures<sup>9–11</sup> and the molecular geometry<sup>8,12</sup> of *n*-C<sub>44</sub>H<sub>90</sub>, tetratetracontane (TTC), adsorbed on noble metals. In the infrared reflection absorption (IRA) spectra for TTC physisorbed on Ag(111) and Au(111) surfaces,<sup>12</sup> lowering of the CH stretching vibration frequency ( $\nu(\text{CH})$ ) was observed.

Such a “softened” CH bond was originally found in the study of cyclic hydrocarbons on catalytically active metals (Ni, Pt, and Ru) by infrared reflection absorption spectroscopy (IRAS) and high-resolution electron energy loss (HREEL) spectroscopy.<sup>13–15</sup> In the HREEL spectrum for cyclohexane on a Ru(001) surface, a shift toward a lower energy of more than 400 cm<sup>-1</sup> from the frequency of the gas phase was observed.<sup>14,16</sup> This frequency lowering of the CH stretching vibration in

cyclohexane adsorbed on Pt, Ni, and Cu has been attributed to a chemical interaction like hydrogen bonding.<sup>17–19</sup> On the other hand, some studies have explained the frequency shift of the  $\nu(\text{CH})$  band on Ru(001) in terms of dipole–image dipole interaction.<sup>14</sup> IRAS studies of *n*-alkanes adsorbed on noble metals (Au, Ag, and Pt) and Cu also showed spectral changes in the CH stretching vibration region from that of the gas phase.<sup>6,7,12,20</sup> However, the origin of the spectral changes and the CH/metal interaction is not yet clear. Yoshinobu et al.<sup>20</sup> investigated methane adsorbed on Pt(111) using IRAS and temperature-programmed desorption and showed that physisorption causes a reduction in the symmetry of methane from *T<sub>d</sub>* to *C<sub>3v</sub>* probably due to softening of one of the four CH bonds. A similar spectral change was reported in a system where the CH bond is in a quite different chemical environment, exemplified by a CH/CD mixture of alkane.<sup>21,22</sup> Unfortunately, the mechanism of the vibrational spectral changes of hydrocarbons due to physisorption has not yet been discussed in detail.

As part of our systematic studies of TTC on various metal surfaces, in this work we studied TTC adsorbed on a Ag(111) surface and on a polycrystalline Cu surface. For TTC on a Ag(111) surface, we found a significant lowering of the  $\nu(\text{CH})$  vibration frequency, which indicates that the electromagnetic interaction is considerable when the CH group is very close to the metal surface. Although similar softening was observed for TTC on Au(111), as reported in the preceding paper,<sup>8</sup> the results for a Au(111) surface were rather complex owing to the appearance of several structures. In contrast, the present results for Ag(111) were simple with regard to structural aspects, making them suitable for a detailed analysis of the effect of CH/metal interaction. With the aid of information about the nature of adsorption<sup>9,10</sup> and following the formalism reported by other workers,<sup>23–25</sup> we analyzed the observed results and developed an electrodynamic model based on the interaction between the transition dipole and the image dipole produced by conduction electrons at the metal surface. The results

\* Corresponding author.

<sup>†</sup> Department of Chemistry.

<sup>‡</sup> Research Center for Materials Science.

<sup>§</sup> Present address: Department of Chemistry, College of Arts and Sciences, Showa University, 1-5-8 Hatanodai, Shinagawa-ku, Tokyo 142-8555, Japan. Facsimile: +81-3-3784-8258. E-mail: yama@cas.showa-u.ac.jp.

<sup>⊥</sup> Present address: Department of Information Processing, Interdisciplinary Graduate School of Science and Engineering, Tokyo Institute of Technology, 4259 Nagatsuta, Midori-ku, Yokohama 226-8502, Japan.

gave a semiquantitative explanation of the softening of the CH bond.

## II. Experimental Section

The apparatus used for measuring IRA spectra has been described in the preceding paper.<sup>8</sup> Briefly, it consists of a Fourier transform IR spectrometer, a mercury cadmium telluride detector, and an ultrahigh vacuum (UHV) chamber (the base pressure was below  $5 \times 10^{-10}$  Torr) equipped with bakeable ZnSe windows and a LEED–Auger electron spectroscopy (AES) system. The optical path outside of the UHV chamber was purged with  $\text{H}_2\text{O}$ -free air generated by a dry air system (Airtech AT-35HD). Samples were prepared and measured in-situ in the UHV chamber.

First, the Au(111) surface for the IRA measurement was prepared by vacuum evaporation on a freshly cleaved mica substrate ( $23 \times 10$  mm). The Ag(111) surface for the IRA measurement was then prepared by vacuum evaporation on the Au(111) surface. The evaporation of Au and Ag was carried out by resistive heating using a W wire and an electron bombardment evaporation source (OMICRON EFM4), respectively. The temperature of the substrate was controlled by resistive heating of a Si plate attached to the back of the mica substrate. The substrate was kept at ca. 260 °C during the evaporation and was annealed at the same temperature for 15 min after the evaporation of Au and Ag. LEED and AES measurements verified the successful preparation of clean Au(111) and Ag(111) surfaces. The Auger electron signals of carbon or oxygen contamination were below the detection limit. The evaporation of Cu on a hydrogen-terminated Si substrate<sup>26</sup> ( $11 \times 5$  mm) was carried out by resistive heating of W wire. The substrate was kept at room temperature during evaporation.

TTC was purchased from Tokyo Chemical Industry Co. Ltd. and was purified by recrystallization from benzene. After a reference spectrum was taken with a clean metal surface, TTC was deposited on the surface in a stepwise manner and an IRA spectrum was measured at each step. The deposition of TTC was performed using a quartz crucible with a resistive heater, which was located 125 mm from the substrate. The substrate was maintained at room temperature during the deposition.

The IRA spectra were obtained in a single-reflection mode with p-polarized light at an angle of incidence  $80^\circ$  relative to the surface normal. One thousand scans were averaged in a total measurement time of 5 min with a resolution of  $4\text{ cm}^{-1}$ . We estimated the thickness of the TTC film by a quartz microbalance, which showed a constant evaporation rate of  $0.02\text{ Å/s}$ . Here we express the thickness by evaporation time in seconds. The intensities and frequencies of the IRA bands were obtained through peak separation by curve-fitting processes using Lorentzian functions.

## III. Results and Discussion

**III.A. IRA Spectra for TTC on Ag(111).** The changes in the IRA spectra with the evaporation of TTC on the Ag(111) surface are summarized in Figure 1. In the spectrum at an evaporation time of 16 s, IRA bands at 2907 and  $2814\text{ cm}^{-1}$  are observed and their intensities change with the evaporation time, as shown in Figure 2. Up to an evaporation time of 87 s, the two peaks are observed without any change in frequencies. An evaporation time of 87 s, when the  $2907\text{-cm}^{-1}$  band shows its maximum intensity, corresponds to an average thickness of about 2 Å. Judging from the thickness, these bands are attributed to the adsorbates on the Ag(111) surface that form the first layer.

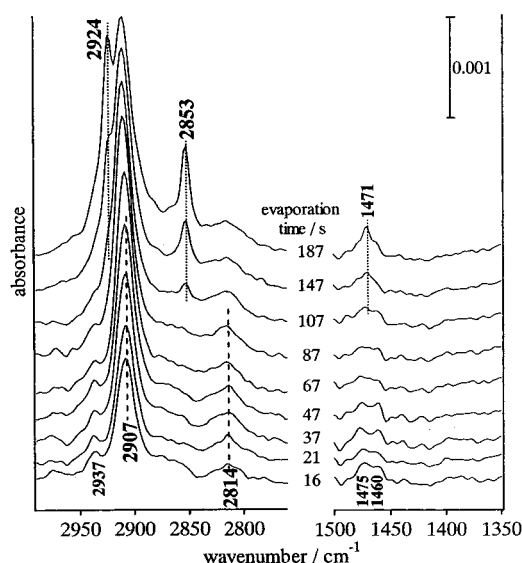


**Figure 1.** IRA spectra with the evaporation of TTC on Ag(111). The evaporation time in seconds is shown at the center of each spectrum.

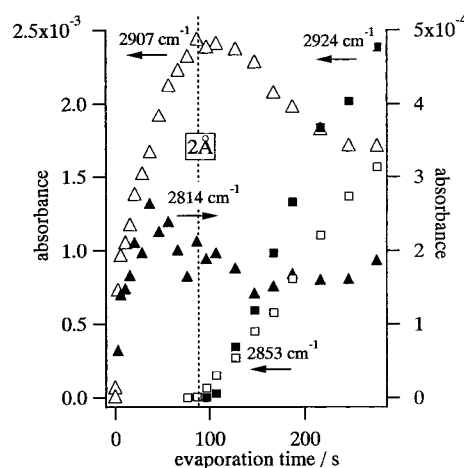


**Figure 2.** Changes in the absorbance intensity of the IRA bands in Figure 1 at  $2907\text{ cm}^{-1}$  (HC/Ag,  $\Delta$ ),  $2814\text{ cm}^{-1}$  (CH/Ag,  $\blacktriangle$ ),  $2924\text{ cm}^{-1}$  ( $\nu_{\text{as}}(\text{CH}_2)$ ,  $\blacksquare$ ), and  $2853\text{ cm}^{-1}$  ( $\nu_{\text{s}}(\text{CH}_2)$ ,  $\square$ ) with the evaporation time in seconds. Number on the dashed line indicates the thickness in Å of the TTC film when the  $2907\text{-cm}^{-1}$  band shows the maximum intensity.

This first layer also gives the other IRA bands at 2937, 1475, and  $1460\text{ cm}^{-1}$  in Figure 1.

In the spectrum at an evaporation time of 107 s, new bands clearly appear at 2924, 2853, and  $1471\text{ cm}^{-1}$ . These bands are assigned to the  $\text{CH}_2$  antisymmetric stretching vibration ( $\nu_{\text{as}}(\text{CH}_2)$ ),  $\text{CH}_2$  symmetric stretching vibration ( $\nu_{\text{s}}(\text{CH}_2)$ ), and  $\text{CH}_2$  scissoring vibration ( $\delta(\text{CH}_2)$ ) of the methylene group, respectively.<sup>21</sup> As shown in Figure 2, after an evaporation time of 100 s, the intensities of the  $\nu_{\text{as}}(\text{CH}_2)$  and  $\nu_{\text{s}}(\text{CH}_2)$  bands increase linearly with further evaporation. We ascribe the appearance of these bands to the formation of a new structure of TTC in addition to that in the first layer. The simultaneous appearance of  $\nu_{\text{as}}(\text{CH}_2)$  and  $\nu_{\text{s}}(\text{CH}_2)$  bands shows that this structure includes methylene groups tilted to the surface, and the frequencies of these IRA bands indicate that the structure includes a *gauche* conformation.<sup>27</sup> The details of such structures, which were also observed for TTC on a Au(111) surface, are discussed in the preceding paper.<sup>8</sup>

**III.B. Flat-on Geometry of TTC.** TTC in the first structure on the Ag(111) surface gives two IRA bands at 2814 and  $2907\text{ cm}^{-1}$ , while the second structure gives  $\nu_{\text{as}}(\text{CH}_2)$  and  $\nu_{\text{s}}(\text{CH}_2)$

bands at 2924 and 2853  $\text{cm}^{-1}$ . The former spectral pattern for the TTC adsorbate is much different from that of bulk TTC, which mainly shows a combination of symmetric and antisymmetric bands of the methylene group in the CH stretching vibration region. When the molecular plane formed by the C atoms of extended TTC is parallel to the surface, all of the methylene groups in the TTC can contact the surface through one of the two H atoms in the methylene group. If the two CH bonds in the methylene group are no longer equivalent, the molecular plane of the extended TTC is not a plane of symmetry. The reduction in symmetry from an extended TTC ( $C_{2h}$ ) to a flat TTC on the surface ( $C_2$ ) reduces the coupling between the two originally equivalent CH stretching vibrations in a methylene group, leading to the appearance of two independent CH stretching vibration ( $\nu(\text{CH})$ ) bands instead of  $\nu_{\text{as}}(\text{CH}_2)$  and  $\nu_{\text{s}}(\text{CH}_2)$  bands. Considering these two features in the spectrum of the first layer, we suppose that the TTC adsorbed on the Ag surface assumes a "flat-on" structure, where the molecular plane is parallel to the surface. Very similar results were obtained for a TTC/Au(111) system, though one of the two  $\nu(\text{CH})$  bands is supposed to be shifted and broadened to the extent that it is difficult to detect it.<sup>8</sup>

In this flat-on structure, the two IRA bands at 2907 and 2814  $\text{cm}^{-1}$  are attributed mainly to the CH bonds in the upper side of the molecular plane (hereafter denoted as HC/Ag) and those in the vicinity of the Ag(111) surface (CH/Ag), respectively.<sup>12</sup> The 2907- $\text{cm}^{-1}$  band (HC/Ag) is similar in energy to the "isolated" CH stretching vibration of the methylene group, which was observed for CH/CD blended bulk alkanes in the region of 2892–2920  $\text{cm}^{-1}$ .<sup>21,22</sup> The 2814- $\text{cm}^{-1}$  band (CH/Ag) is ascribed to the CH vibration perturbed by the Ag surface. Similar softened CH stretching vibration bands of hexane and pentane on Cu(111) surfaces were also observed at 2808  $\text{cm}^{-1}$ .<sup>7</sup> Thus, we adopt the expression  $\nu(\text{CH})$  for the 2907- and 2814- $\text{cm}^{-1}$  bands in Figure 1, rather than  $\nu_{\text{as}}(\text{CH}_2)$  and  $\nu_{\text{s}}(\text{CH}_2)$ . The details of the supposed decoupling will be discussed later. The  $\text{CH}_2$  bending bands at 1475 and 1460  $\text{cm}^{-1}$  in Figure 1 are not so strong in intensity, and we do not think that their overtone bands affect the 2908- $\text{cm}^{-1}$  band. Furthermore, we could not find any experimental results indicating that the 2814- $\text{cm}^{-1}$  band is affected by overtones or Fermi resonance.<sup>28,29</sup> The 2937- $\text{cm}^{-1}$  band in Figure 1 is also similar in energy to the isolated CH stretching vibration of the terminal methyl group, which was observed in CH/CD blended bulk.<sup>21, 22</sup>

For comparison with the spectra in Figure 1, we show the IRA spectra for TTC adsorbates on Au(111) and Cu surfaces in Figure 3. The TTCs on both surfaces at room temperature give only one strong IRA band around 2910  $\text{cm}^{-1}$ , which is assigned to  $\nu(\text{CH})$  or  $\nu_{\text{as}}(\text{CH}_2)$ . As possible reasons for why the spectra do not show the  $\nu_{\text{s}}(\text{CH}_2)$  band at 2840–2855  $\text{cm}^{-1}$ , we can consider the above-described reduction in symmetry or the surface selection rule of IRAS.<sup>25,30</sup> The latter states that IRAS enables us to selectively observe vibrations whose transition moments are perpendicular to the metal surface. Since in the  $\nu_{\text{s}}(\text{CH}_2)$  mode the transition moment is parallel to the molecular plane, TTC adsorbed with its molecular plane parallel to the surface does not show the  $\nu_{\text{s}}(\text{CH}_2)$  band in its IRA spectra. In either case, Figure 3 shows that TTCs on Au(111) and Cu surfaces at room temperature assume a flat-on geometry. The spectral features of the CH/Au(111) system were explained in the preceding paper.<sup>8</sup>

**III.C.  $\nu(\text{CH})$  Bands Perturbed by Au and Ag Surfaces.** As shown in Figure 3, the spectra of TTC deposited on a Au(111) surface at room temperature change with temperature and

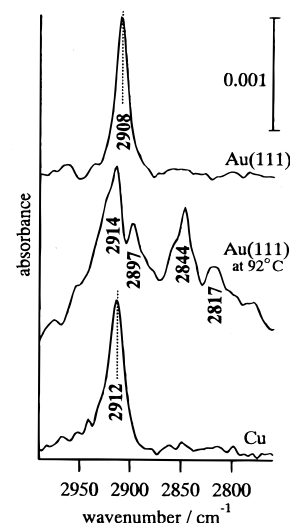


**Figure 3.** IRA spectra for TTC adsorbed on Au(111) and Cu surfaces. The temperature of the sample substrate in  $^{\circ}\text{C}$  is indicated on the right of a spectrum, while the other spectra without numbers were measured at room temperature.

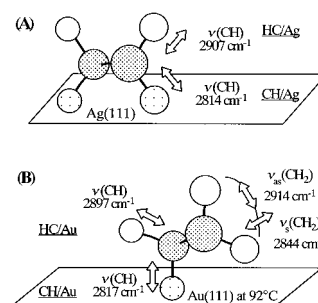


**Figure 4.** (A) Two  $\text{CH}_2$  groups of flat-on TTC on Ag(111) and (B) those of tilted TTC on Au(111) at 92  $^{\circ}\text{C}$ .

give IRA bands at 2914, 2897, 2844, and 2817  $\text{cm}^{-1}$  at 92  $^{\circ}\text{C}$ . The two IRA bands at 2914 and 2844  $\text{cm}^{-1}$  are assigned to the  $\nu_{\text{as}}(\text{CH}_2)$  and  $\nu_{\text{s}}(\text{CH}_2)$  bands of the normal methylene group, respectively. The two other IRA bands at 2897 and 2817  $\text{cm}^{-1}$  are attributed to the methylene group interacting with the Au(111) surface.<sup>8</sup> The appearance of two types of methylene groups suggests that the molecular plane of TTC is tilted to the surface. The two kinds of methylene groups are that on the far side from the Au(111) surface and that in the vicinity of the surface, respectively.<sup>8,12</sup>

We summarize the assignments of these IRA bands and the geometries of "flat-on TTC" on Ag(111) and "tilted TTC" on Au(111) at 92  $^{\circ}\text{C}$  in Figure 4. The methylene group in the vicinity of Au(111) has two different CH groups. One directly interacts with the surface (CH/Au), which should mainly give the 2817- $\text{cm}^{-1}$  band. The other is the isolated CH group (HC/Au), which should contribute to the 2897- $\text{cm}^{-1}$  band. As shown in Figures 1 and 3, the ratio of the intensity of the 2814- $\text{cm}^{-1}$  band (CH/Ag) to that of the 2907- $\text{cm}^{-1}$  band (HC/Ag) is lower than that of the intensity of the 2817- $\text{cm}^{-1}$  band (CH/Au) to that of the 2897- $\text{cm}^{-1}$  band (HC/Au). This is explained by the orientation of the CH axis and the surface selection rule of IRAS. We can see that the appearance of the softened  $\nu$  band around 2815  $\text{cm}^{-1}$  depends on the surfaces and the orientation of the methylene group.

**III.D. CH–Metal Interaction.** While CH–metal interaction for hydrocarbons is still controversial, the mechanism of the changes in the spectra for CO/metal systems has been discussed in detail.<sup>31</sup> There are reportedly three main reasons for the



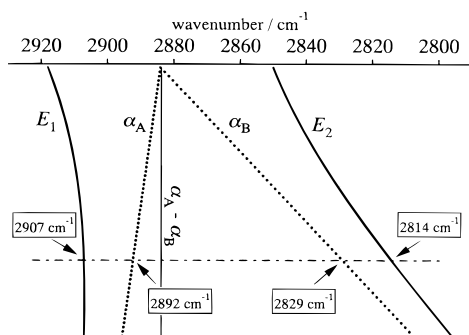


**Figure 5.** Relationships of the parameters  $E_1$ ,  $E_2$ ,  $\alpha_A$ , and  $\alpha_B$  to the difference  $\alpha_A - \alpha_B$  between the two CH stretching vibrations.

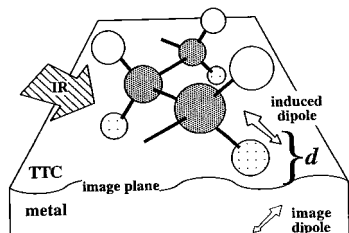


**Figure 6.** Some TTC in a flat-on geometry on a metal surface and the CH group interacting with its image dipole.  $d$  is the distance between the dipole of a CH group and the image plane.

frequency shift of the CO stretching ( $\nu(\text{CO})$ ) vibration on metals, i.e., (1) electron transfer between the adsorbate and the metal (e.g., back-donation to CO), (2) lateral dipole–dipole interaction among the adsorbates, and (3) dipole–image dipole interaction with the metal. We will examine whether such factors can contribute to the shift of the  $\nu$  band to a lower frequency.

A study on the electronic structure of TTC on Au and Ag surfaces by metastable atom electron (MAE) spectroscopy showed that the spectral feature corresponding to the highest occupied molecular orbital (HOMO) energy is independent of the TTC thickness.<sup>9,10</sup> The adsorption energy per a CH<sub>2</sub> group in *n*-alkanes on a Cu(100) was estimated to be about 6 kJ/mol, indicating physisorption.<sup>32</sup> From these results, we can deduce that the TTCs that give the spectra in Figures 1, 2, and 3 are physisorbed on Au(111), Ag(111), and Cu, and that there will be little electron transfer between TTC and these metals.

Some IRAS studies on CO/metal have revealed strong shifts of the  $\nu(\text{CO})$  band to a higher frequency with increasing coverage. This shift was ascribed to lateral dipole–dipole interaction among the adsorbates.<sup>24,30,31</sup> As shown in Figure 1, the  $\nu$  bands of flat-on TTC at 2907 and 2814 cm<sup>−1</sup> show no frequency shift in the early stage of evaporation (at a thickness of 0.3–1.3 Å). This indicates that lateral dipole–dipole interaction among flat-on TTCs does not contribute to the frequency shifts.

The last possible origin is dipole–dipole interaction with the image dipole produced in the metal. Figure 6 illustrates a part of TTC in a flat-on geometry on a metal surface and the CH group interacting with its image dipole. We will examine whether this factor can explain the observed results by model calculations.

**III.E. Model Calculation of the Image Effect. III.E.1. Decoupling.** First we need to know the bare energy for the vibration of an isolated CH bond ( $\nu(\text{CH})$ ). To estimate the degree of decoupling of two CH stretching modes in a methylene group, we assume that a wave function  $\psi$  for a state with an observed vibrational energy can be expressed by a linear combination of wave functions,  $\psi(\text{A})$  and  $\psi(\text{B})$ , which indicate

the states of two isolated CH stretching vibrations in the methylene group:

$$\psi = C_A \psi(\text{A}) + C_B \psi(\text{B}) \quad (1)$$

Using the variation principle, we can find the coefficients  $C_A$  and  $C_B$  through secular equations and the secular determinant<sup>33</sup>

$$\begin{vmatrix} \alpha_A - E & \beta \\ \beta & \alpha_B - E \end{vmatrix} = 0 \quad (2)$$

where  $E$  is the observed vibrational energy and  $\alpha_A$  and  $\alpha_B$  are the energies for the two isolated CH stretching vibrations, respectively.  $\beta$  is a parameter related to the coupling. Its solution can be expressed in terms of a parameter  $\xi$ , as

$$\cot 2\xi = (\alpha_A - \alpha_B)/2\beta \quad (3)$$

where  $x$  indicates the degree of the coupling effect. The solutions are

$$\psi = (\cos \xi)\psi(\text{A}) + (\sin \xi)\psi(\text{B}) \quad E = \alpha_B + \beta \cot \xi \quad (4)$$

$$\psi = -(\sin \xi)\psi(\text{A}) + (\cos \xi)\psi(\text{B}), \quad E = \alpha_A - \beta \cot \xi \quad (5)$$

The strongest coupling is obtained when the two CH vibrations have the same energy. We regard the typical  $\nu_{\text{as}}(\text{CH}_2)$  and  $\nu_{\text{s}}(\text{CH}_2)$  vibration bands observed at 2918 and 2850 cm<sup>−1</sup> as perfect coupling modes.<sup>8</sup> In this case, the parameters are  $E_1 = 2918$  cm<sup>−1</sup>,  $E_2 = 2850$  cm<sup>−1</sup>,  $\alpha_A = \alpha_B = (E_1 + E_2)/2 = 2884$  cm<sup>−1</sup> and  $\beta = (E_1 - E_2)/2 = 34$  cm<sup>−1</sup>. On the other hand, in the case of flat-on TTC, we observed  $E_1$  and  $E_2$  at 2907 and 2814 cm<sup>−1</sup>, respectively. According to the above equations and using  $\beta = 34$  cm<sup>−1</sup>, we found the parameters  $\alpha_A = 2892$  cm<sup>−1</sup>,  $\alpha_B = 2829$  cm<sup>−1</sup>, and  $\xi = 23.49^\circ$ . These values give

$$\psi_1 = 0.9171\psi(\text{A}) + 0.3986\psi(\text{B}), \quad E_1 = 2907 \text{ cm}^{-1} \quad (6)$$

$$\psi_2 = -0.3986\psi(\text{A}) + 0.9171\psi(\text{B}), \quad E_2 = 2814 \text{ cm}^{-1} \quad (7)$$

We summarize the relationship between the difference  $\alpha_A - \alpha_B$  and the parameters  $E_1$ ,  $E_2$ ,  $\alpha_A$ , and  $\alpha_B$  in Figure 5. An important feature is that as the difference  $\alpha_A - \alpha_B$  between the two CH stretching vibrations increases, the value of  $\xi$  decreases. When the energy difference is large, the energies of the CH stretching vibrations differ only slightly from those of the isolated CH stretching vibrations, which implies that the coupling effects are small, as seen in eqs 6 and 7. Thus, we choose the description  $\nu(\text{CH})$ s for the 2907- and 2814-cm<sup>−1</sup> bands rather than  $\nu_{\text{as}}(\text{CH}_2)$  and  $\nu_{\text{s}}(\text{CH}_2)$ . In the following calculations, we will use the parameters  $\alpha_A = 2892$  cm<sup>−1</sup> and  $\alpha_B = 2829$  cm<sup>−1</sup> as the frequencies of pure HC/Ag and CH/Ag in the methylene group, respectively.

**III.E.2. Formulation.** We regard TTC as a dielectric medium, which has no strong chemical interaction (charge transfer or chemical bonding) with Ag. A CH group is regarded as a harmonic oscillator and is treated as a point dipole, on the supposition that the  $\nu(\text{CH})$  mode consists of the sum of the motions of the individual CH bonds and does not couple with other normal modes in a TTC molecule. The dipole consists of carbon and hydrogen, and their motions induce the transition dipole moment. We do not account for the contribution from the dipoles in the neighboring methylene groups and their respective image dipoles, whether they are in the same molecule or in the neighboring TTC. This is because the two-dimensional geometry<sup>2</sup> of the flat *n*-alkane on Ag(111) shows that these

dipoles are away from each other at intervals of more than 2 Å, making their effect much smaller than its own image effect within the range of interest, as shown below. Retardation of the field from the surrounding dipoles is neglected because the wavelength of infrared radiation is much larger than the area of interest.

We regard a CH group as an independent dipole, which has a polarizability  $\alpha(\omega)$  at frequency  $\omega$ . The total dipole moment  $p(\omega)$  of the adsorbed CH at an adsorption site of Ag(111) is thus given by

$$p(\omega) = p_{\text{st}} + \alpha(\omega) E^{\text{loc}} \quad (8)$$

The first term  $p_{\text{st}}$  is the static dipole moment of a CH group without the image effect by the metal surface. The second term shows that the induced oscillating dipole moment is proportional to the local electric field  $E^{\text{loc}}(\omega)$  at the adsorption site. The local field is the sum of the incident macroscopic field  $E$  and the field due to its own image dipole  $E^{\text{image}}$ :

$$E^{\text{loc}} = E + E^{\text{image}} \quad (9)$$

As shown in Figure 6, the field  $E^{\text{image}}$  comes from the image dipole, which is located at a distance  $2d$  from the original dipole, where  $d$  is the distance between the original dipole and the image plane produced by the Ag surface. Since the image dipole has the same dipole moment  $p(\omega)$  as the original one,  $E^{\text{image}}$  is given by<sup>33</sup>

$$E^{\text{image}} = p(\omega)/4d^3 \quad (10)$$

Combination of eqs 8–10 yields

$$p(\omega) = \{p_{\text{st}}/[1 - \alpha(\omega)/(4d^3)]\} + \{\alpha(\omega)/[1 - \alpha(\omega)/(4d^3)]\} E \quad (11)$$

The second term can be regarded as the oscillating dipole moment  $p_{\text{ind}}(\omega)$  induced by the field  $E$ . The change in the polarizable CH group on the Ag surface from that in a vacuum is shown by the modification of polarizability  $\alpha(\omega)$  to effective polarizability  $\alpha_{\text{eff}}(\omega)$ . These relations can be expressed as

$$p_{\text{ind}}(\omega) = \alpha_{\text{eff}}(\omega) E(\omega) \quad (12)$$

$$\alpha_{\text{eff}}(\omega) = \alpha(\omega)/[1 - \alpha(\omega)/(4d^3)] \quad (13)$$

The polarizability  $\alpha(\omega)$  arises from the distortion of the electron clouds and the displacement of the cores of the CH group. Thus, the polarizability  $\alpha(\omega)$  is the sum of an electronic part  $\alpha_e$  due to electronic polarization, including the contribution from valence and core electrons, and a vibrational part  $\alpha_v$  caused by vibration of the atomic cores. The electronic part is independent of frequency in the range of interest, and the vibrational part is supposed to have a single Lorentzian line shape<sup>23–25</sup>

$$\alpha(\omega) = \alpha_e + \alpha_v(\omega) \quad (14)$$

$$\alpha_v(\omega) = [e^{*2}/(4\pi^2\mu\omega_0^2)]/[1 - (\omega/\omega_0)^2 + i\gamma(\omega/\omega_0)] \quad (15)$$

where  $\omega_0$  is the resonant frequency,  $e^*$  the effective charge,  $\mu$  the reduced mass, and  $\gamma\omega_0$  the line width.

The change in reflectivity  $(R^0 - R)/R^0$  arising from the presence of an adsorbed surface layer on metal is proportional to the imaginary part of the effective polarizability  $\alpha_{\text{eff}}(\omega)$ .<sup>24,25</sup>  $R$  and  $R^0$  are the reflectivities of the metal substrate with and

without the adsorbate, respectively. Thus, we obtain

$$(R^0 - R)/R^0 \sim \omega N \text{Im}\{\alpha_{\text{eff}}(\omega)\} \quad (16)$$

where  $N$  is the number of adsorbates per unit area. The frequency of an IRA band corresponds to the position of a minimum value of eq 16, and the shift from frequency  $\omega_0$  is explained by the modification of polarizability. Next, we will examine the numerical values for the parameters in these equations.

**III.E.3. Parameters.** In the case of CO/metal, parameter  $\omega_0$  was obtained from the frequency of the stretching vibration for the limit of zero coverage on the surface.<sup>24</sup> This value is smaller than that of the gas phase, since the CO bond of the adsorbate becomes weak owing to back-donation from the metal surface. On the other hand, the TTC/Ag system lacks strong chemical bonding to Ag. Thus, we can regard parameter  $\omega_0$  as the frequency of the isolated  $\nu(\text{CH})$  mode, which is free from chemical interaction with the surface. The frequencies of the isolated  $\nu(\text{CH})$  bands in the methylene groups observed for CH/CD blended bulk alkane were around 2900  $\text{cm}^{-1}$ .<sup>21,22</sup> We regard the value of parameter  $\omega_0$  as 2884  $\text{cm}^{-1}$ , which is the average energy of typical  $\nu_{\text{as}}(\text{CH}_2)$  and  $\nu_{\text{s}}(\text{CH}_2)$  vibration bands observed at 2918 and 2850  $\text{cm}^{-1}$ , respectively.<sup>8</sup> We determined the line width  $\gamma\omega_0 = 27.3 \text{ cm}^{-1}$  by the experimental results in Figure 1. The values of  $\omega_0$  and  $\gamma$  are not sensitive to the magnitude of the shift, but only to the absolute frequency and to the width of the peak, respectively.

The vibrational part of the polarizability along the CH bond can be determined to be  $1.25 \times 10^{-3}/[1 - (\omega/\omega_0)^2 + i\gamma(\omega/\omega_0)] \text{ Å}^3$  by eq 15, using the value  $e^{*2}/(\mu\omega_0^2) = (0.05e)^2/[0.93 \text{ u} (2884 \text{ cm}^{-1})^2]$  for the  $\nu(\text{CH})$  band derived from the IR absorption intensity.<sup>34,35</sup> This value is for motion along the CH axis. We use the vertical component of the parameter since we observe only the transition moment perpendicular to the surface owing to the surface selection rule of IRAS. The CH bond in flat-on TTC is inclined at an angle of 36° from the surface normal. Transformation of the coordinate system leads to a vertical component  $\alpha_v = 8.5 \times 10^{-4}/[1 - (\omega/\omega_0)^2 + i\gamma(\omega/\omega_0)] \text{ Å}^3$  as the vibrational part of the polarizability. The electronic part of polarizability  $\alpha_e$  can be obtained by subtracting  $e^{*2}/(\mu\omega_0^2)$  (a part of  $\alpha_v$  shown in eq 15) from the total polarizability.<sup>23,24</sup> The values of the total polarizability for ethane and propane in a direction perpendicular to the molecular axes are 3.97 and 6.93  $\text{Å}^3$ , respectively.<sup>36</sup> Half of the difference between them is 1.48  $\text{Å}^3$ , which can be regarded as the value of the total polarizability for a CH group. Considering the small value of the numerator of  $\alpha_v$  ( $e^{*2}/(\mu\omega_0^2)$ ) compared with that of the total polarizability, the value of the electronic part  $\alpha_e$  for CH/Ag was supposed to be 1.5  $\text{Å}^3$ . Owing to the possibility of errors, we showed the frequency dependence on  $\alpha_e$  using a value of  $\alpha_e = 1.5 \pm 0.3 \text{ Å}^3$ .

**III.E.4. Calculation.** To estimate the dipole–image dipole interaction, we take the distance  $d$  between the induced dipole of the CH stretching vibration and the image plane as a variable parameter. The correlation between the frequency of the  $\nu(\text{CH})$  band in wavenumber and the parameter  $d$  in Å is summarized in Figure 7. The calculated frequencies converge to 2884  $\text{cm}^{-1}$  at  $d > 0.85 \text{ Å}$ . As  $d$  decreases below 0.80 Å, the  $\nu(\text{CH})$  bands show abrupt downward shifts in their frequency. A sudden change occurs at larger  $d$ , as  $\alpha_e$  becomes large. If we ascribe the frequency difference between 2884  $\text{cm}^{-1}$  (free isolated CH) and 2829  $\text{cm}^{-1}$  (CH/Ag) to the variation in  $d$ , 2829  $\text{cm}^{-1}$  corresponds to  $d = 0.72 \text{ Å}$  when  $\alpha_e$  is 1.5  $\text{Å}^3$ , and 2884  $\text{cm}^{-1}$  corresponds to  $d > 0.85 \text{ Å}$ . At  $d > 0.85 \text{ Å}$ , there is no

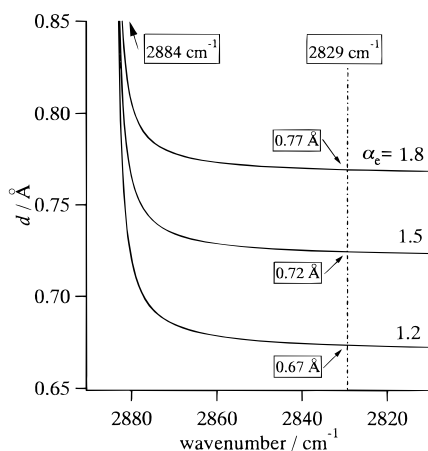


**Figure 7.** Simulated correlation between the frequency of the  $\nu(\text{CH})$  band and the distance  $d$  from the point dipole to the effective image plane. Numbers on the right side indicate the electronic component of the polarizability  $\alpha_e$  in  $\text{\AA}^3$ .

contribution from the image dipole, and this suggests that the dipole–dipole interaction among lateral dipoles more than 2  $\text{\AA}$  from each other is negligible.

The direction and magnitude of the simulated shift are reasonable, if the value of  $d$  is less than 0.8  $\text{\AA}$ . Theoretical and experimental studies on methane physisorbed on Pt have given an estimated equilibrium distance for the H atom on Pt of 2–3  $\text{\AA}$ .<sup>37,38</sup> Unfortunately, the distance  $d$  between the induced point dipole and the effective image plane is different from the distance between cores of atoms, and the location of the image plane is not well defined owing to tailing of the metal electrons into vacuum. When the CH group is well fitted into the hollow site, the point dipole can come very close to the effective image plane.<sup>14</sup> In the case of CO/metal, the frequency of the  $\nu(\text{CO})$  band for the adsorbate in the hollow site is much lower than that in the atop site.<sup>39</sup> Scheffler explained the vibrational spectra of the CO/Pd(100) system using the dipole–dipole coupling mechanism with  $d = 0.96 \text{ \AA}$ .<sup>24</sup> This value is smaller than 1.5–1.9  $\text{\AA}$  for the distance between the C atom of adsorbed CO and the surface plane composed of centers of metal atoms.<sup>39</sup> Since an H atom is smaller than a C atom, we think that the  $d$  value 0.67–0.77  $\text{\AA}$  is possible for the TTC/Ag(111) system under a good geometrical fit.

As shown in LEED studies,<sup>2</sup> all of the CHs/Ag of  $n$ -alkane in a flat-on geometry cannot be at a hollow site of Ag atoms on the (111) surface. This incommensurate relation between CH groups and Ag atoms may have produced the dispersion of the value of  $d$ . This may be why the 2814- $\text{cm}^{-1}$  band is broad and the peak absorbance is low. This also explains the difference in the evaporation time corresponding to the maximum intensities of the 2907- and 2814- $\text{cm}^{-1}$  bands in Figure 2.

In theory, the total area intensity of the perturbed  $\nu(\text{CH})$  bands assigned to all kinds of CHs/Ag should be equal to that of the HCs/Ag (the 2907- $\text{cm}^{-1}$  band in Figure 1). To examine this point, we are now preparing IRAS and LEED measurements of TTC adsorbed on a better-defined single-crystal surface with high sensitivity. In the present study, however, we observed only one perturbed  $\nu(\text{CH})$  band assigned to one kind of CH/Ag at 2814  $\text{cm}^{-1}$  in Figure 1. Therefore, a single value of  $d$  was used in this simulation, corresponding to a single representative adsorption site of the Ag(111) surface.

The  $\nu(\text{CH})$  bands at 2907 and 2814  $\text{cm}^{-1}$  have been explained only by electromagnetic interaction between the induced dipole of the CH group and its image dipole, on the assumption that electron transfer does not occur between the molecule and the

surface. Recently, C1s core excitation spectra of alkanes on metals have suggested the possibility of a change in the electronic structure even by physisorption.<sup>40</sup> Actually, the vibrational spectra for adsorbates depend on metals and surfaces.<sup>39,41</sup> Further investigation should be focused on the detailed correlation between the vibrational properties and the electronic structure at molecule–metal interfaces.

#### IV. Conclusion

In this study, we found that TTC is adsorbed on Ag(111) with the molecular plane parallel to the surface, and the IRA spectra gave two  $\nu(\text{CH})$  bands at 2907 and 2814  $\text{cm}^{-1}$ . We suppose that the CH bond in the lower frequency vibration is perturbed by the Ag surface. On the other hand, the MAE spectra did not show a shift of the HOMO level of the TTC molecule, suggesting that the CH group is not chemically bound to the surface. This “CH softened” mode was explained in terms of dipole–image dipole interaction with the Ag surface. The frequency was simulated by electrodynamic calculations with  $d$ , the distance between the induced dipole of the CH stretching vibration and the effective image plane at the Ag surface. The perturbed  $\nu(\text{CH})$  band observed at 2814  $\text{cm}^{-1}$  was explained with  $d = 0.67\text{--}0.77 \text{ \AA}$  for the CH group in the vicinity of the Ag surface.

**Acknowledgment.** M.Y. acknowledges the support of Research Fellowships for Young Scientists from the Japan Society for the Promotion of Science. This work was supported in part by Grants-in-Aid for Scientific Research from the Ministry of Education, Science, Sports and Culture of Japan (Nos.10440205 and 07CE2004) and also by the Venture Business Laboratory Program “High Performance Nanoprocess Technology” of Nagoya University.

#### References and Notes

- (1) Firment, L. E.; Somorjai, G. A. *J. Chem. Phys.* **1977**, *66*, 2901.
- (2) Firment, L. E.; Somorjai, G. A. *J. Chem. Phys.* **1978**, *69*, 3940.
- (3) Luongo, J. P.; Schonhorn, H. *J. Polym. Sci., Part A2* **1968**, *6*, 1649.
- (4) Chan, M. G.; Allara, D. L. *Polym. Eng. Sci.* **1974**, *14*, 12.
- (5) Sack, S.; Schar, S.; Steger, E. *Polym. Degrad. Stab.* **1984**, *7*, 193.
- (6) Chesters, M. A.; Gardner, P.; McCash, E. M. *Surf. Sci.* **1989**, *209*, 89.
- (7) Teplyakov, A. V.; Bent, B. E.; Eng, J. J.; Chen, J. G. *Surf. Sci.* **1998**, *399*, L342.
- (8) Yamamoto, M.; Sakurai, Y.; Hosoi, Y.; Ishii, H.; Kajikawa, K.; Ouchi, Y.; Seki, K. *J. Phys. Chem. B* **2000**, 7363.
- (9) Ito, E. Ph.D. Thesis, Nagoya University, Nagoya, Japan, 1997; pp 110–131.
- (10) Ito, E.; Oji, H.; Ishii, H.; Oichi, K.; Ouchi, Y.; Seki, K. *Chem. Phys. Lett.* **1998**, *287*, 137.
- (11) Yoshimura, D.; Ishii, H.; Ouchi, Y.; Ito, E.; Miyamae, T.; Hasegawa, S.; Okudaira, K. K.; Ueno, N.; Seki, K. *Phys. Rev. B* **1999**, *60*, 9046.
- (12) Yamamoto, M.; Sakurai, Y.; Hosoi, Y.; Ishii, H.; Ito, E.; Kajikawa, K.; Ouchi, Y.; Seki, K. *Surf. Sci.* **1999**, *427–428*, 388.
- (13) Demuth, J. E.; Ibach, H.; Lehwald, S. *Phys. Rev. Lett.* **1978**, *40*, 1044.
- (14) Hoffmann, F. M.; Upton, T. H. *J. Phys. Chem.* **1984**, *88*, 6209.
- (15) Sheppard, N. *Annu. Rev. Phys. Chem.* **1988**, *39*, 589.
- (16) Madey, T. E.; Yates, J. J. T. *Surf. Sci.* **1978**, *76*, 397.
- (17) Raval, R.; Chesters, M. A. *Surf. Sci.* **1989**, *219*, L505.
- (18) Lamont, C. L. A.; Borbach, M.; Martin, R.; Gardner, P.; Jones, T. S.; Conrad, H.; Bradshaw, A. M. *Surf. Sci.* **1997**, *374*, 215.
- (19) Wang, J.; MacBreen, P. H. *Surf. Sci.* **1997**, *392*, L45.
- (20) Yoshinobu, J.; Ogasawara, H.; Kawai, M. *Phys. Rev. Lett.* **1995**, *75*, 2176.
- (21) MacPhail, R. A.; Strauss, H. L.; Snyder, R. G.; Elliger, C. A. *J. Phys. Chem.* **1984**, *88*, 334.
- (22) Snyder, R. G.; Aljibury, A. L.; Strauss, H. L.; Casal, H. L.; Gough, K. M.; Murphy, W. E. *J. Chem. Phys.* **1984**, *81*, 5352.
- (23) Mahan, G. D.; Lucas, A. *J. Chem. Phys.* **1978**, *68*, 1344.
- (24) Scheffler, M. *Surf. Sci.* **1979**, *81*, 562.

- (25) Chabal, Y. J. *Surf. Sci. Rep.* **1988**, 8, 211.
- (26) Higashi, G. S.; Becker, R. S.; Chabal, Y. J.; Becker, A. J. *Appl. Phys. Lett.* **1991**, 58, 1656.
- (27) Snyder, R. G. *J. Chem. Phys.* **1967**, 47, 1316.
- (28) Snyder, R. G.; Hsu, S. L.; Krimm, S. *Spectrochim. Acta A* **1978**, 34, 395.
- (29) Snyder, R. G.; Scherer, J. R. *J. Chem. Phys.* **1979**, 71, 3221.
- (30) Sučaka, W. *Surface Infrared and Raman Spectroscopy*; Methods of Surface Characterization, Vol. 3; Plenum: New York, 1995; Chapter 2, pp 13–115.
- (31) Hoffmann, F. M. *Surf. Sci. Rep.* **1983**, 3, 107.
- (32) Sexton, B. A.; Hughes, A. E. *Surf. Sci.* **1984**, 140, 227.
- (33) Atkins, P. W. *Physical Chemistry*; Oxford University Press: Oxford, 1992.
- (34) Francis, S. A. *J. Chem. Phys.* **1950**, 18, 861.
- (35) Ibach, H. *Surf. Sci.* **1977**, 66, 56.
- (36) Hirschfelder, J. O.; Curtiss, C. F.; Bird, R. B. *Molecular Theory of Gases and Liquids*; John Wiley & Sons: New York, 1963.
- (37) Akinaga, Y.; Taketsugu, T.; Hirao, K. *J. Chem. Phys.* **1997**, 107, 415.
- (38) Matsumoto, Y.; Gruzdkov, Y. A.; Watanabe, K.; Sawabe, K. *J. Chem. Phys.* **1996**, 105, 4775.
- (39) Somorjai, G. A. *Introduction to Surface Chemistry and Catalysis*; John Wiley & Sons: New York, 1994; Chapter 4, pp 319–361.
- (40) Weiss, K.; Weckesser, J.; Wöll, C. *J. Mol. Struct.* **1999**, 458, 143.
- (41) Strunskus, T.; Grunze, M.; Kochendoerfer, G.; Wöll, C. *Langmuir* **1996**, 12, 2712.